POLITECNICO DI TORINO
Repository ISTITUZIONALE

Analysis of laminated shells by a sinusoidalshear deformation theory and Radial Basis Functions collocation, accounting for through-the-thickness deformations.

Original
Analysis of laminated shells by a sinusoidalshear deformation theory and Radial Basis Functions collocation, accounting for through-the-thickness deformations / Ferreira, A. J. M.; Roque, C. C.; Carrera, Erasmo; Cinefra, Maria; Polit, O.. - In: COMPOSITES. PART B, ENGINEERING. - ISSN 1359-8368. - 42:(2011), pp. 1276-1284. [10.1016/j.compositesb.2011.01.031]

Availability:
This version is available at: 11583/2381148 since:

Publisher:
Elsevier

Published
DOI:10.1016/j.compositesb.2011.01.031

Terms of use:

This article is made available under terms and conditions as specified in the corresponding bibliographic description in the repository

Publisher copyright

(Article begins on next page)

28 April 2024

Analysis of laminated shells by a sinusoidal shear deformation theory and radial basis functions collocation, accounting for through-the-thickness deformations

A.J.M. Ferreira [a,*], E. Carrera [c], M. Cinefra [c], C.M.C. Roque [b], O. Polit [d]

[a] Departamento de Engenharia Mecânica, Faculdade de Engenharia da, Universidade do Porto, Rua Dr. Roberto Frias, 4200-465 Porto, Portugal
[b] INEGI, Faculdade de Engenharia da Universidade do Porto, Rua Dr. Roberto Frias, 4200-465 Porto, Portugal
[c] Departament of Aeronautics and Aerospace Engineering, Politecnico di Torino, Corso Duca degli Abruzzi, 24, 10129 Torino, Italy
[d] Université Paris Ouest – Nanterre, 50 rue de Sevres, 92410 Ville d'Avray, France

A B S T R A C T

In this paper, the static and free vibration analysis of laminated shells is performed by radial basis functions collocation, according to a sinusoidal shear deformation theory (SSDT). The SSDT theory accounts for through-the-thickness deformation, by considering a sinusoidal evolution of all displacements with the thickness coordinate. The equations of motion and the boundary conditions are obtained by the Carrera's Unified Formulation, and further interpolated by collocation with radial basis functions.

1. Introduction

The efficient load-carrying capabilities of shell structures make them very useful in a variety of engineering applications. The continuous development of new structural materials leads to ever increasingly complex structural designs that require careful analysis. Although analytical techniques are very important, the use of numerical methods to solve shell mathematical models of complex structures has become an essential ingredient in the design process.

The most common mathematical models used to describe shell structures may be classified in two classes according to different physical assumptions: the Koiter model [1], based on the Kirchhoff hypothesis and the Naghdi model [2], based on the Reissner–Mindlin assumptions that take into account the transverse shear deformation. In this paper, the Unified Formulation (UF) by Carrera [3–8] is proposed to derive the equations of motion and boundary conditions. This formulation contains a large variety of 2D models that differ in the order of used expansion in thickness direction and in the manner the variables are modelled along the thickness. In particular, the UF is here applied to analyse laminated shells by radial basis functions (RBF) collocation, according to a sinus-based shear deformation theory that accounts for through-the-thickness deformations. This theory is an expansion of the developments by Touratier [9–11], and Vidal and Polit [12]. It allows a sinusoidal variation of all displacement components along the thickness and it is more convenient than the classical Taylor polynomials because the sine function can be expressed by means of Taylor expansion. Moreover, the derivative of displacements in the deformations does not reduce the order of the approximating functions. The choice of the sine function can be justified from the three-dimensional point of view, using the work of Cheng [13]. As it can be seen in Polit [14], a sine term appears in the solution of the shear equation (see Eq. (7) in [2]). Therefore, the kinematics proposed can be seen as an approximation of the exact three-dimensional solution. Furthermore, the sine function has an infinite radius of convergence and its Taylor expansion includes not only the third-order terms but all the odd terms.

The most common numerical procedure for the analysis of the shells is the finite element method [15–19]. It is known that the phenomenon of numerical locking may arise from hidden constrains that are not well represented in the finite element approximation and, in scientific literature, it is possible to find many methods to overcome this problem [20–25]. The present paper, that performs the bending and free vibration analysis of laminated shells by collocation with radial basis functions, avoids the locking phenomenon. A radial basis function, $\phi(\|x - x_j\|)$ is a spline that depends on the Euclidian distance between distinct data centers $x_{j,j} = 1, 2, \ldots, N \in \mathbb{R}^n$, also called nodal or collocation points. The

so-called unsymmetrical Kansa method, introduced by Kansa [26], is employed. The use of radial basis function for the analysis of structures and materials has been previously studied by numerous authors [27–41]. The authors have recently applied the RBF collocation to the static deformations of composite beams and plates [42–44].

In this paper it is investigated for the first time how the Unified Formulation can be combined with radial basis functions to the analysis of thin and thick laminated shells, using the SSDT, allowing for through-the-thickness deformations. The quality of the present method in predicting static deformations and free vibrations of thin and thick laminated shells is compared and discussed with other methods in some numerical examples.

2. Applying the Unified Formulation to SSDT

The Unified Formulation proposed by Carrera, also known as CUF, is a powerful framework for the analysis of beams, plates and shells. This formulation has been applied in several finite element analysis, either using the Principle of Virtual Displacements, or by using the Reissner's Mixed Variational theorem. The stiffness matrix components, the external force terms or the inertia terms can be obtained directly with this UF, irrespective of the shear deformation theory being considered.

In this section, it is shown how to obtain the fundamental nuclei, which allows the derivation of the equations of motion and boundary conditions according to CUF, in weak form for the finite element analysis and in strong form for the present RBF collocation.

3. A sinus shear deformation theory

The present sinus shear deformation theory involves the following expansion of displacements

$$u = u_0 + zu_1 + \sin\left(\frac{\pi z}{h}\right)u_3; \quad v = v_0 + zv_1 + \sin\left(\frac{\pi z}{h}\right)v_3; \quad w = w_0 + zw_1 + \sin\left(\frac{\pi z}{h}\right)w_3 \tag{1}$$

where u_0, v_0 and w_0 are translations of a point at the middle-surface of the plate, and u_1, v_1, u_3, v_3 denote rotations. This theory is an expansion of early developments by Touratier [9–11], and Vidal and Polit [12]. It considers a sinusoidal variation of all displacements u, v, w, allowing for through-the-thickness deformations. Extension to shells becomes evident in the next sections.

3.1. Governing equations and boundary conditions in the framework of Unified Formulation

Shells are bi-dimensional structures in which one dimension (in general the thickness in z direction) is negligible with respect to the other two in-plane dimensions. Geometry and the reference system are indicated in Fig. 1. The square of an infinitesimal linear segment in the layer, the associated infinitesimal area and volume are given by:

$$\begin{aligned} ds_k^2 &= H_\alpha^{k\,2}\,d\alpha^2 + H_\beta^{k\,2}\,d\beta^2 + H_z^{k\,2}\,dz^2 \\ d\Omega_k &= H_\alpha^k H_\beta^k\,d\alpha\,d\beta \\ dV &= H_\alpha^k H_\beta^k H_z^k\,d\alpha\,d\beta\,dz \end{aligned} \tag{2}$$

where the metric coefficients are:

$$H_\alpha^k = A^k(1 + z/R_\alpha^k), \quad H_\beta^k = B^k(1 + z/R_\beta^k), \quad H_z^k = 1 \tag{3}$$

k denotes the k-layer of the multilayered shell; R_α^k and R_β^k are the principal radii of curvature along the coordinates α and β, respectively. A^k and B^k are the coefficients of the first fundamental form of Ω_k (Γ_k is the Ω_k boundary). In this work, the attention has been restricted to shells with constant radii of curvature (cylindrical, spherical, toroidal geometries) for which $A^k = B^k = 1$.

Although one can use the UF for one-layer, isotropic shell, a multi-layered shell with N_l layers is considered. The Principle of Virtual Displacements (PVD) for the pure-mechanical case reads:

$$\sum_{k=1}^{N_l}\int_{\Omega_k}\int_{A_k}\left\{\delta\epsilon_{pG}^{k\,T}\sigma_{pC}^k + \delta\epsilon_{nG}^{k\,T}\sigma_{nC}^k\right\}d\Omega_k\,dz = \sum_{k=1}^{N_l}\delta L_e^k \tag{4}$$

where Ω_k and A_k are the integration domains in plane (α,β) and z direction, respectively. Here, k indicates the layer and T the transpose of a vector, and δL_e^k is the external work for the kth layer. G means geometrical relations and C constitutive equations.

The steps to obtain the governing equations are:

- Substitution of the geometrical relations (subscript G).
- Substitution of the appropriate constitutive equations (subscript C).
- Introduction of the Unified Formulation.

Stresses and strains are separated into in-plane and normal components, denoted, respectively, by the subscripts p and n. The mechanical strains in the kth layer can be related to the displacement field $\mathbf{u}^k = \{u_\alpha^k, u_\beta^k, u_z^k\}$ via the geometrical relations:

$$\begin{aligned} \epsilon_{pG}^k &= [\epsilon_{\alpha\alpha}^k, \epsilon_{\beta\beta}^k, \epsilon_{\alpha\beta}^k]^T = (\boldsymbol{D}_p^k + \boldsymbol{A}_p^k)\boldsymbol{u}^k, \quad \epsilon_{nG}^k = [\epsilon_{\alpha z}^k, \epsilon_{\beta z}^k, \epsilon_{zz}^k]^T \\ &= (\boldsymbol{D}_{n\Omega}^k + \boldsymbol{D}_{nz}^k - \boldsymbol{A}_n^k)\boldsymbol{u}^k \end{aligned} \tag{5}$$

The explicit form of the introduced arrays follows:

$$\boldsymbol{D}_p^k = \begin{bmatrix} \frac{\partial_\alpha}{H_\alpha^k} & 0 & 0 \\ 0 & \frac{\partial_\beta}{H_\beta^k} & 0 \\ \frac{\partial_\beta}{H_\beta^k} & \frac{\partial_\alpha}{H_\alpha^k} & 0 \end{bmatrix}, \quad \boldsymbol{D}_{n\Omega}^k = \begin{bmatrix} 0 & 0 & \frac{\partial_\alpha}{H_\alpha^k} \\ 0 & 0 & \frac{\partial_\beta}{H_\beta^k} \\ 0 & 0 & 0 \end{bmatrix}, \quad \boldsymbol{D}_{nz}^k = \begin{bmatrix} \partial_z & 0 & 0 \\ 0 & \partial_z & 0 \\ 0 & 0 & \partial_z \end{bmatrix}, \tag{6}$$

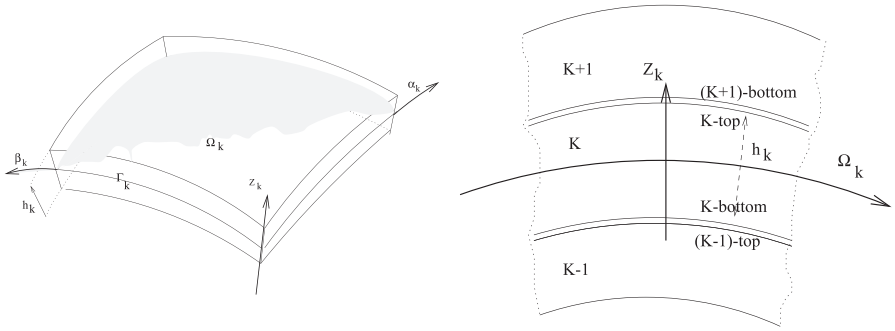

Fig. 1. Geometry and notations for a multilayered shell (doubly curved).

$$\boldsymbol{A}_p^k = \begin{bmatrix} 0 & 0 & \frac{1}{H_\alpha^k R_\alpha^k} \\ 0 & 0 & \frac{1}{H_\beta^k R_\beta^k} \\ 0 & 0 & 0 \end{bmatrix}, \quad \boldsymbol{A}_n^k = \begin{bmatrix} \frac{1}{H_\alpha^k R_\alpha^k} & 0 & 0 \\ 0 & \frac{1}{H_\beta^k R_\beta^k} & 0 \\ 0 & 0 & 0 \end{bmatrix} \tag{7}$$

The 3D constitutive equations are given as:

$$\begin{aligned} \sigma_{pC}^k &= \mathbf{C}_{pp}^k \epsilon_{pG}^k + \mathbf{C}_{pn}^k \epsilon_{nG}^k \\ \sigma_{nC}^k &= \mathbf{C}_{np}^k \epsilon_{pG}^k + \mathbf{C}_{nn}^k \epsilon_{nG}^k \end{aligned} \tag{8}$$

with

$$\begin{aligned} \mathbf{C}_{pp}^k &= \begin{bmatrix} C_{11}^k & C_{12}^k & C_{16}^k \\ C_{12}^k & C_{22}^k & C_{26}^k \\ C_{16}^k & C_{26}^k & C_{66}^k \end{bmatrix}, \quad \mathbf{C}_{pn}^k = \begin{bmatrix} 0 & 0 & C_{13}^k \\ 0 & 0 & C_{23}^k \\ 0 & 0 & C_{36}^k \end{bmatrix}, \\ \mathbf{C}_{np}^k &= \begin{bmatrix} 0 & 0 & 0 \\ 0 & 0 & 0 \\ C_{13}^k & C_{23}^k & C_{36}^k \end{bmatrix}, \quad \mathbf{C}_{nn}^k = \begin{bmatrix} C_{55}^k & C_{45}^k & 0 \\ C_{45}^k & C_{44}^k & 0 \\ 0 & 0 & C_{33}^k \end{bmatrix} \end{aligned} \tag{9}$$

According to the Unified Formulation by Carrera, the three displacement components u_α, u_β and u_z and their relative variations can be modelled as:

$$\begin{aligned} (u_\alpha, u_\beta, u_z) &= F_\tau(u_{\alpha\tau}, u_{\beta\tau}, u_{z\tau}), \quad (\delta u_\alpha, \delta u_\beta, \delta u_z) \\ &= F_s(\delta u_{\alpha s}, \delta u_{\beta s}, \delta u_{zs}) \end{aligned} \tag{10}$$

where the F_τ are functions of the thickness coordinate z and τ is a sum index. Taylor expansions from first- up to fourth-order are employed: $F_0 = z^0 = 1$, $F_1 = z^1 = z, \ldots, F_N = z^N, \ldots, F_4 = z^4$ if an Equivalent Single Layer (ESL) model is used. For ESL approach, one means that the displacements are assumed for the whole laminate if a multilayer structure is considered.

Resorting to the displacement field in Eq. (10), the vectors $F_t = \begin{bmatrix} 1 & z & \sin\left(\frac{\pi z}{h}\right) \end{bmatrix}$ are chosen for the displacements u, v, w. Then, all the terms of the equations of motion are obtained by integrating through the thickness direction.

It is interesting to note that under this combination of the Unified Formulation and RBF collocation, the collocation code depends only on the choice of F_t, in order to solve this type of problems. A MATLAB code has been designed that, just by changing F_t, can analyse static deformations, and free vibrations for any type of C^∞ shear deformation theory. An obvious advantage of the present methodology is that the tedious derivation of the equations of motion and boundary conditions for a particular shear deformation theory is no longer an issue, as this MATLAB code does all that work for us.

In Fig. 2, it is shown the assembling procedures of the stiffness matrix on layer k for the ESL approach.

Substituting the geometrical relations, the constitutive equations and the Unified Formulation into the variational statement PVD, for the kth layer, one has:

$$\begin{aligned} &\sum_{k=1}^{N_l} \left\{ \int_{\Omega_k} \int_{A_k} \left\{ \left((\boldsymbol{D}_p + \boldsymbol{A}_p) \delta \boldsymbol{u}^k \right)^T \left(\mathbf{C}_{pp}^k (\boldsymbol{D}_p + \boldsymbol{A}_p) \boldsymbol{u}^k + \mathbf{C}_{pn}^k (\boldsymbol{D}_{n\Omega} + \boldsymbol{D}_{nz} - \boldsymbol{A}_n) \boldsymbol{u}^k \right) \right. \right. \\ &+ \left((\boldsymbol{D}_{n\Omega} + \boldsymbol{D}_{nz} - \boldsymbol{A}_n) \delta \boldsymbol{u}^k \right)^T \left(\mathbf{C}_{np}^k (\boldsymbol{D}_p + \boldsymbol{A}_p) \boldsymbol{u}^k \right. \\ &\left. \left. \left. + \mathbf{C}_{nn}^k (\boldsymbol{D}_{n\Omega} + \boldsymbol{D}_{nz} - \boldsymbol{A}_n) \boldsymbol{u}^k \right) \right\} d\Omega_k dz_k \right\} = \sum_{k=1}^{N_l} \delta L_e^k \end{aligned} \tag{11}$$

At this point, the formula of integration by parts is applied:

$$\begin{aligned} \int_{\Omega_k} \left((\mathbf{D}_\Omega) \delta \mathbf{a}^k \right)^T \mathbf{a}^k d\Omega_k = &- \int_{\Omega_k} \delta \mathbf{a}^{kT} \left((\mathbf{D}_\Omega^T) \mathbf{a}^k \right) d\Omega_k \\ &+ \int_{\Gamma_k} \delta \mathbf{a}^{kT} \left((\mathbf{I}_\Omega) \mathbf{a}^k \right) d\Gamma_k \end{aligned} \tag{12}$$

where $\mathbf{I}_\Omega$ matrix is obtained applying the *Gradient theorem*:

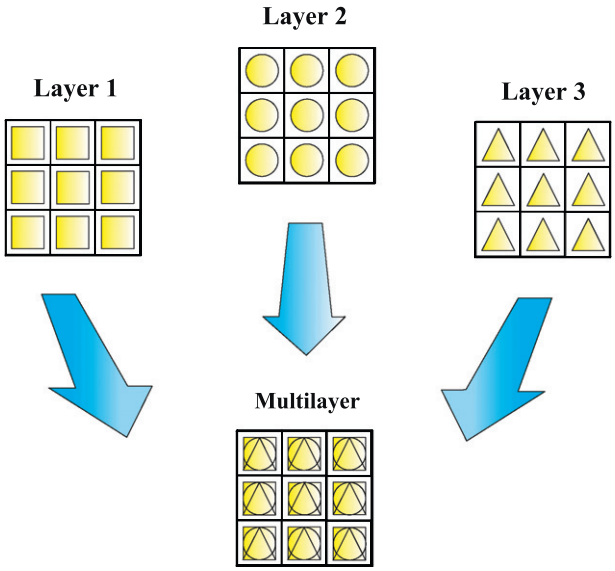

Fig. 2. Assembling procedure for ESL approach.

$$\int_\Omega \frac{\partial \psi}{\partial x_i} d\upsilon = \oint_\Gamma n_i \psi \, ds \tag{13}$$

being n_i the components of the normal $\hat{n}$ to the boundary along the direction i. After integration by parts and the substitution of CUF, the governing equations and boundary conditions for the shell in the mechanical case are obtained:

$$\begin{aligned} &\sum_{k=1}^{N_l} \left\{ \int_{\Omega_k} \int_{A_k} \left\{ \delta \boldsymbol{u}_s^{kT} \left[(-\boldsymbol{D}_p + \boldsymbol{A}_p)^T F_s (\mathbf{C}_{pp}^k (\boldsymbol{D}_p + \boldsymbol{A}_p) F_\tau \boldsymbol{u}_\tau^k \right. \right. \right. \\ &+ \mathbf{C}_{pn}^k (\boldsymbol{D}_{n\Omega} + \boldsymbol{D}_{nz} - \boldsymbol{A}_n) F_\tau \boldsymbol{u}_\tau^k) \left. \right] \\ &+ \delta \boldsymbol{u}_s^{kT} \left[(-\boldsymbol{D}_{n\Omega} + \boldsymbol{D}_{nz} - \boldsymbol{A}_n)^T F_s (\mathbf{C}_{np}^k (\boldsymbol{D}_p + \boldsymbol{A}_p) F_\tau \boldsymbol{u}_\tau^k \right. \\ &\left. \left. \left. + \mathbf{C}_{nn}^k (\boldsymbol{D}_{n\Omega} + \boldsymbol{D}_{nz} - \boldsymbol{A}_n) F_\tau \boldsymbol{u}_\tau^k) \right] \right\} d\Omega_k dz_k \right\} \\ &+ \sum_{k=1}^{N_l} \left\{ \int_{\Gamma_k} \int_{A_k} \left\{ \delta \boldsymbol{u}_s^{kT} \left[\boldsymbol{I}_p^T F_s (\mathbf{C}_{pp}^k (\boldsymbol{D}_p + \boldsymbol{A}_p) F_\tau \boldsymbol{u}_\tau^k \right. \right. \right. \\ &+ \mathbf{C}_{pn}^k (\boldsymbol{D}_{n\Omega} + \boldsymbol{D}_{nz} - \boldsymbol{A}_n) F_\tau \boldsymbol{u}_\tau^k) \left. \right] + \delta \boldsymbol{u}_s^{kT} \left[\boldsymbol{I}_{np}^T F_s (\mathbf{C}_{np}^k (\boldsymbol{D}_p - \boldsymbol{A}_p) F_\tau \boldsymbol{u}_\tau^k \right. \\ &\left. \left. \left. + \mathbf{C}_{nn}^k (\boldsymbol{D}_{n\Omega} + \boldsymbol{D}_{nz} - \boldsymbol{A}_n) F_\tau \boldsymbol{u}_\tau^k) \right] \right\} d\Gamma_k dz_k \right\} = \sum_{k=1}^{N_l} \left\{ \int_{\Omega_k} \delta \boldsymbol{u}_s^{kT} F_s \boldsymbol{p}_u^k \right\} \end{aligned} \tag{14}$$

where $\mathbf{I}_p^k$ and $\mathbf{I}_{np}^k$ depend on the boundary geometry:

$$\mathbf{I}_p = \begin{bmatrix} \frac{n_\alpha}{H_\alpha} & 0 & 0 \\ 0 & \frac{n_\beta}{H_\beta} & 0 \\ \frac{n_\beta}{H_\beta} & \frac{n_\alpha}{H_\alpha} & 0 \end{bmatrix}; \quad \mathbf{I}_{np} = \begin{bmatrix} 0 & 0 & \frac{n_\alpha}{H_\alpha} \\ 0 & 0 & \frac{n_\beta}{H_\beta} \\ 0 & 0 & 0 \end{bmatrix} \tag{15}$$

The normal to the boundary of domain Ω is:

$$\hat{\boldsymbol{n}} = \begin{bmatrix} n_\alpha \\ n_\beta \end{bmatrix} = \begin{bmatrix} cos(\varphi_\alpha) \\ cos(\varphi_\beta) \end{bmatrix} \tag{16}$$

where φ_α and φ_β are the angles between the normal $\hat{n}$ and the direction α and β, respectively.

The governing equations for a multi-layered shell subjected to mechanical loadings are:

$$\delta \mathbf{u}_s^{k^T} : \mathbf{K}_{uu}^{k\tau s} \mathbf{u}_\tau^k = \mathbf{P}_{u\tau}^k \tag{17}$$

where the fundamental nucleus $\mathbf{K}_{uu}^{k\tau s}$ is obtained as:

$$\boldsymbol{K}_{uu}^{k\tau s}=\int_{A_k}\Big[[-\boldsymbol{D}_p+\boldsymbol{A}_p]^T\boldsymbol{C}_{pp}^k[\boldsymbol{D}_p+\boldsymbol{A}_p]+[-\boldsymbol{D}_p+\boldsymbol{A}_p]^T\boldsymbol{C}_{pn}^k[\boldsymbol{D}_{n\Omega}+\boldsymbol{D}_{nz}-\boldsymbol{A}_n]+[-\boldsymbol{D}_{n\Omega}+\boldsymbol{D}_{nz}-\boldsymbol{A}_n]^T\boldsymbol{C}_{np}^k[\boldsymbol{D}_p+\boldsymbol{A}_p]+[-\boldsymbol{D}_{n\Omega}+\boldsymbol{D}_{nz}-\boldsymbol{A}_n]^T\boldsymbol{C}_{nn}^k[\boldsymbol{D}_{n\Omega}+\boldsymbol{D}_{nz}-\boldsymbol{A}_n]\Big]F_\tau F_s H_\alpha^k H_\beta^k dz \tag{18}$$

and the corresponding Neumann-type boundary conditions on Γ_k are:

$$\boldsymbol{\Pi}_d^{k\tau s}\mathbf{u}_\tau^k=\boldsymbol{\Pi}_d^{k\tau s}\bar{\mathbf{u}}_\tau^k \tag{19}$$

where

$$\boldsymbol{\Pi}_d^{k\tau s}=\int_{A_k}\Big[\boldsymbol{I}_p^T\boldsymbol{C}_{pp}^k[\boldsymbol{D}_p+\boldsymbol{A}_p^\tau]+\boldsymbol{I}_p^T\boldsymbol{C}_{pn}^k[\boldsymbol{D}_{n\Omega}+\boldsymbol{D}_{nz}-\boldsymbol{A}_n^\tau]+\boldsymbol{I}_{np}^T\boldsymbol{C}_{np}^k[\boldsymbol{D}_p+\boldsymbol{A}_p^\tau]+\boldsymbol{I}_{np}^T\boldsymbol{C}_{nn}^k[\boldsymbol{D}_{n\Omega}+\boldsymbol{D}_{nz}-\boldsymbol{A}_n^\tau]\Big]F_\tau F_s H_\alpha^k H_\beta^k dz \tag{20}$$

and $\mathbf{P}_{u\tau}^k$ are variationally consistent loads with applied pressure.

3.2. Fundamental nuclei

The following integrals are introduced to perform the explicit form of fundamental nuclei:

$$\begin{aligned}
&\Big(J^{k\tau s},J_\alpha^{k\tau s},J_\beta^{k\tau s},J_{\frac{\alpha}{\beta}}^{k\tau s},J_{\frac{\beta}{\alpha}}^{k\tau s},J_{\alpha\beta}^{k\tau s}\Big)=\int_{A_k}F_\tau F_s\Big(1,H_\alpha,H_\beta,\frac{H_\alpha}{H_\beta},\frac{H_\beta}{H_\alpha},H_\alpha H_\beta\Big)dz\\
&\Big(J^{k\tau_z s},J_\alpha^{k\tau_z s},J_\beta^{k\tau_z s},J_{\frac{\alpha}{\beta}}^{k\tau_z s},J_{\frac{\beta}{\alpha}}^{k\tau_z s},J_{\alpha\beta}^{k\tau_z s}\Big)=\int_{A_k}\frac{\partial F_\tau}{\partial z}F_s\Big(1,H_\alpha,H_\beta,\frac{H_\alpha}{H_\beta},\frac{H_\beta}{H_\alpha},H_\alpha H_\beta\Big)dz\\
&\Big(J^{k\tau s_z},J_\alpha^{k\tau s_z},J_\beta^{k\tau s_z},J_{\frac{\alpha}{\beta}}^{k\tau s_z},J_{\frac{\beta}{\alpha}}^{k\tau s_z},J_{\alpha\beta}^{k\tau s_z}\Big)=\int_{A_k}F_\tau\frac{\partial F_s}{\partial z}\Big(1,H_\alpha,H_\beta,\frac{H_\alpha}{H_\beta},\frac{H_\beta}{H_\alpha},H_\alpha H_\beta\Big)dz\\
&\Big(J^{k\tau_z s_z},J_\alpha^{k\tau_z s_z},J_\beta^{k\tau_z s_z},J_{\frac{\alpha}{\beta}}^{k\tau_z s_z},J_{\frac{\beta}{\alpha}}^{k\tau_z s_z},J_{\alpha\beta}^{k\tau_z s_z}\Big)=\int_{A_k}\frac{\partial F_\tau}{\partial z}\frac{\partial F_s}{\partial z}\\
&\Big(1,H_\alpha,H_\beta,\frac{H_\alpha}{H_\beta},\frac{H_\beta}{H_\alpha},H_\alpha H_\beta\Big)dz
\end{aligned}\tag{21}$$

The fundamental nuclei $\mathbf{K}_{uu}^{k\tau s}$ is reported for doubly curved shells (radii of curvature in both α and β directions (see Fig. 1)):

$$\begin{aligned}
\Big(\mathbf{K}_{uu}^{\tau sk}\Big)_{11}&=-C_{11}^k J_{\beta/\alpha}^{k\tau s}\partial_\alpha^s\partial_\alpha^\tau-C_{16}^k J^{k\tau s}\partial_\alpha^\tau\partial_\beta^s-C_{16}^k J^{k\tau s}\partial_\alpha^s\partial_\beta^\tau-C_{66}^k J_{\alpha/\beta}^{k\tau s}\partial_\beta^s\partial_\beta^\tau\\
&\quad+C_{55}^k\Big(J_{\alpha\beta}^{k\tau_z s_z}-\frac{1}{R_{\alpha_k}}J_\beta^{k\tau_z s}-\frac{1}{R_{\alpha_k}}J_\beta^{k\tau s_z}+\frac{1}{R_{\alpha_k}^2}J_{\beta/\alpha}^{k\tau s}\Big)\\
\Big(\mathbf{K}_{uu}^{\tau sk}\Big)_{12}&=-C_{12}^k J^{k\tau s}\partial_\alpha^\tau\partial_\beta^s-C_{16}^k J_{\beta/\alpha}^{k\tau s}\partial_\alpha^s\partial_\alpha^\tau-C_{26}^k J_{\alpha/\beta}^{k\tau s}\partial_\beta^s\partial_\beta^\tau-C_{66}^k J^{k\tau s}\partial_\alpha^s\partial_\beta^\tau\\
&\quad+C_{45}^k\Big(J_{\alpha\beta}^{k\tau_z s_z}-\frac{1}{R_{\beta_k}}J_\alpha^{k\tau_z s}-\frac{1}{R_{\alpha_k}}J_\beta^{k\tau s_z}+\frac{1}{R_{\alpha_k}}\frac{1}{R_{\beta_k}}J^{k\tau s}\Big)\\
\Big(\mathbf{K}_{uu}^{\tau sk}\Big)_{13}&=-C_{11}^k\frac{1}{R_{\alpha_k}}J_{\beta/\alpha}^{k\tau s}\partial_\alpha^\tau-C_{12}^k\frac{1}{R_{\beta_k}}J^{k\tau s}\partial_\alpha^\tau-C_{13}^k J_\beta^{k\tau s_z}\partial_\alpha^\tau-C_{16}^k\frac{1}{R_{\alpha_k}}J^{k\tau s}\partial_\beta^\tau\\
&\quad-C_{26}^k\frac{1}{R_{\beta_k}}J_{\alpha/\beta}^{k\tau s}\partial_\beta^\tau-C_{36}^k J_\alpha^{k\tau s_z}\partial_\beta^\tau+C_{45}^k\Big(J_\alpha^{k\tau_z s}\partial_\beta^s-\frac{1}{R_{\alpha_k}}J^{k\tau s}\partial_\beta^s\Big)\\
&\quad+C_{55}^k\Big(J_\beta^{k\tau_z s}\partial_\alpha^s-\frac{1}{R_{\alpha_k}}J_{\beta/\alpha}^{k\tau s}\partial_\alpha^s\Big)\\
\Big(\mathbf{K}_{uu}^{\tau sk}\Big)_{21}&=-C_{12}^k J^{k\tau s}\partial_\alpha^s\partial_\beta^\tau-C_{16}^k J_{\beta/\alpha}^{k\tau s}\partial_\alpha^s\partial_\alpha^\tau-C_{26}^k J_{\alpha/\beta}^{k\tau s}\partial_\beta^s\partial_\beta^\tau-C_{66}^k J^{k\tau s}\partial_\alpha^\tau\partial_\beta^s\\
&\quad+C_{45}^k\Big(J_{\alpha\beta}^{k\tau_z s_z}-\frac{1}{R_{\beta_k}}J_\alpha^{k\tau s_z}-\frac{1}{R_{\alpha_k}}J_\beta^{k\tau_z s}+\frac{1}{R_{\alpha_k}}\frac{1}{R_{\beta_k}}J^{k\tau s}\Big)\\
\Big(\mathbf{K}_{uu}^{\tau sk}\Big)_{22}&=-C_{22}^k J_{\alpha/\beta}^{k\tau s}\partial_\beta^s\partial_\beta^\tau-C_{26}^k J^{k\tau s}\partial_\alpha^s\partial_\beta^\tau-C_{26}^k J^{k\tau s}\partial_\alpha^\tau\partial_\beta^s-C_{66}^k J_{\beta/\alpha}^{k\tau s}\partial_\alpha^s\partial_\alpha^\tau\\
&\quad+C_{44}^k\Big(J_{\alpha\beta}^{k\tau_z s_z}-\frac{1}{R_{\beta_k}}J_\alpha^{k\tau_z s}-\frac{1}{R_{\beta_k}}J_\alpha^{k\tau s_z}+\frac{1}{R_{\beta_k}^2}J_{\alpha/\beta}^{k\tau s}\Big)
\end{aligned}$$

$$\begin{aligned}
\Big(\mathbf{K}_{uu}^{\tau sk}\Big)_{23}&=-C_{12}^k\frac{1}{R_{\alpha_k}}J^{k\tau s}\partial_\beta^\tau-C_{22}^k\frac{1}{R_{\beta_k}}J_{\alpha/\beta}^{k\tau s}\partial_\beta^\tau-C_{23}^k J_\alpha^{k\tau s_z}\partial_\beta^\tau-C_{16}^k\\
&\quad\times\frac{1}{R_{\alpha_k}}J_{\beta/\alpha}^{k\tau s}\partial_\alpha^\tau-C_{26}^k\frac{1}{R_{\beta_k}}J^{k\tau s}\partial_\alpha^\tau-C_{36}^k J_\beta^{k\tau s_z}\partial_\alpha^\tau\\
&\quad+C_{45}^k\Big(J_\beta^{k\tau_z s}\partial_\alpha^s-\frac{1}{R_{\beta_k}}J^{k\tau s}\partial_\alpha^s\Big)+C_{44}^k\Big(J_\alpha^{k\tau_z s}\partial_\beta^s-\frac{1}{R_{\beta_k}}J_{\alpha/\beta}^{k\tau s}\partial_\beta^s\Big)\\
\Big(\mathbf{K}_{uu}^{\tau sk}\Big)_{31}&=C_{11}^k\frac{1}{R_{\alpha_k}}J_{\beta/\alpha}^{k\tau s}\partial_\alpha^s+C_{12}^k\frac{1}{R_{\beta_k}}J^{k\tau s}\partial_\alpha^s+C_{13}^k J_\beta^{k\tau_z s}\partial_\alpha^s+C_{16}^k\frac{1}{R_{\alpha_k}}J^{k\tau s}\partial_\beta^s\\
&\quad+C_{26}^k\frac{1}{R_{\beta_k}}J_{\alpha/\beta}^{k\tau s}\partial_\beta^s+C_{36}^k J_\alpha^{k\tau_z s}\partial_\beta^s-C_{45}^k\Big(J_\alpha^{k\tau s_z}\partial_\beta^\tau-\frac{1}{R_{\alpha_k}}J^{k\tau s}\partial_\beta^\tau\Big)\\
&\quad-C_{55}^k\Big(J_\beta^{k\tau s_z}\partial_\alpha^\tau-\frac{1}{R_{\alpha_k}}J_{\beta/\alpha}^{k\tau s}\partial_\alpha^\tau\Big)\\
\Big(\mathbf{K}_{uu}^{\tau sk}\Big)_{32}&=C_{12}^k\frac{1}{R_{\alpha_k}}J^{k\tau s}\partial_\beta^s+C_{22}^k\frac{1}{R_{\beta_k}}J_{\alpha/\beta}^{k\tau s}\partial_\beta^s+C_{23}^k J_\alpha^{k\tau_z s}\partial_\beta^s+C_{16}^k\frac{1}{R_{\alpha_k}}J_{\beta/\alpha}^{k\tau s}\partial_\alpha^s\\
&\quad+C_{26}^k\frac{1}{R_{\beta_k}}J^{k\tau s}\partial_\alpha^s+C_{36}^k J_\beta^{k\tau_z s}\partial_\alpha^s-C_{45}^k\Big(J_\beta^{k\tau s_z}\partial_\alpha^\tau-\frac{1}{R_{\beta_k}}J^{k\tau s}\partial_\alpha^\tau\Big)\\
&\quad-C_{44}^k\Big(J_\alpha^{k\tau s_z}\partial_\beta^\tau-\frac{1}{R_{\beta_k}}J_{\alpha/\beta}^{k\tau s}\partial_\beta^\tau\Big)\\
\Big(\mathbf{K}_{uu}^{\tau sk}\Big)_{33}&=C_{11}^k\frac{1}{R_{\alpha_k}^2}J_{\beta/\alpha}^{k\tau s}+C_{22}^k\frac{1}{R_{\beta_k}^2}J_{\alpha/\beta}^{k\tau s}+C_{33}^k J_{\alpha\beta}^{k\tau_z s_z}+2C_{12}^k\frac{1}{R_{\alpha_k}}\\
&\quad\times\frac{1}{R_{\beta_k}}J^{k\tau s}+C_{13}^k\frac{1}{R_{\alpha_k}}\Big(J_\beta^{k\tau_z s}+J_\beta^{k\tau s_z}\Big)+C_{23}^k\\
&\quad\times\frac{1}{R_{\beta_k}}\Big(J_\alpha^{k\tau_z s}+J_\alpha^{k\tau s_z}\Big)-C_{44}^k J_{\alpha/\beta}^{k\tau s}\partial_\beta^s\partial_\beta^\tau-C_{55}^k J_{\beta/\alpha}^{k\tau s}\partial_\alpha^s\partial_\alpha^\tau\\
&\quad-C_{45}^k J^{k\tau s}\partial_\alpha^s\partial_\beta^\tau-C_{45}^k J^{k\tau s}\partial_\alpha^\tau\partial_\beta^s
\end{aligned}\tag{22}$$

The application of boundary conditions makes use of the fundamental nuclei $\boldsymbol{\Pi}_d$ in the form:

$$\begin{aligned}
(\boldsymbol{\Pi}_{uu}^{\tau sk})_{11}&=n_\alpha C_{11}^k J_{\beta/\alpha}^{k\tau s}\partial_\alpha^s+n_\beta C_{66}^k J_{\alpha/\beta}^{k\tau s}\partial_\beta^s+n_\beta C_{16}^k J^{k\tau s}\partial_\alpha^s+n_\alpha C_{16}^k J^{k\tau s}\partial_\beta^s\\
(\boldsymbol{\Pi}_{uu}^{\tau sk})_{12}&=n_\alpha C_{16}^k J_{\beta/\alpha}^{k\tau s}\partial_\alpha^s+n_\beta C_{26}^k J_{\alpha/\beta}^{k\tau s}\partial_\beta^s+n_\alpha C_{12}^k J^{k\tau s}\partial_\beta^s+n_\beta C_{66}^k J^{k\tau s}\partial_\alpha^s\\
(\boldsymbol{\Pi}_{uu}^{\tau sk})_{13}&=n_\alpha\frac{1}{R_{\alpha k}}C_{11}^k J_{\beta/\alpha}^{k\tau s}+n_\alpha\frac{1}{R_{\beta k}}C_{12}^k J^{k\tau s}+n_\alpha C_{13}^k J_\beta^{k\tau s_z}+n_\beta\frac{1}{R_{\alpha k}}C_{16}^k J^{k\tau s}\\
&\quad+n_\beta\frac{1}{R_{\beta k}}C_{26}^k J_{\alpha/\beta}^{k\tau s}+n_\beta C_{36}^k J_\alpha^{k\tau s_z}\\
(\boldsymbol{\Pi}_{uu}^{\tau sk})_{21}&=n_\alpha C_{16}^k J_{\beta/\alpha}^{k\tau s}\partial_\alpha^s+n_\beta C_{26}^k J_{\alpha/\beta}^{k\tau s}\partial_\beta^s+n_\beta C_{12}^k J^{k\tau s}\partial_\alpha^s+n_\alpha C_{66}^k J^{k\tau s}\partial_\beta^s\\
(\boldsymbol{\Pi}_{uu}^{\tau sk})_{22}&=n_\alpha C_{66}^k J_{\beta/\alpha}^{k\tau s}\partial_\alpha^s+n_\beta C_{22}^k J_{\alpha/\beta}^{k\tau s}\partial_\beta^s+n_\beta C_{26}^k J^{k\tau s}\partial_\alpha^s+n_\alpha C_{26}^k J^{k\tau s}\partial_\beta^s\\
(\boldsymbol{\Pi}_{uu}^{\tau sk})_{23}&=n_\alpha\frac{1}{R_{\alpha k}}C_{16}^k J_{\beta/\alpha}^{k\tau s}+n_\alpha\frac{1}{R_{\beta k}}C_{26}^k J^{k\tau s}+n_\alpha C_{36}^k J_\beta^{k\tau s_z}+n_\beta\frac{1}{R_{\alpha k}}C_{12}^k J^{k\tau s}\\
&\quad+n_\beta\frac{1}{R_{\beta k}}C_{22}^k J_{\alpha/\beta}^{k\tau s}+n_\beta C_{23}^k J_\alpha^{k\tau s_z}\\
(\boldsymbol{\Pi}_{uu}^{\tau sk})_{31}&=-n_\alpha\frac{1}{R_{\alpha k}}C_{55}^k J_{\beta/\alpha}^{k\tau s}+n_\alpha C_{55}^k J_\beta^{k\tau s_z}-n_\beta\frac{1}{R_{\alpha k}}C_{45}^k J^{k\tau s}+n_\beta C_{45}^k J_\alpha^{k\tau s_z}\\
(\boldsymbol{\Pi}_{uu}^{\tau sk})_{32}&=-n_\alpha\frac{1}{R_{\beta k}}C_{45}^k J^{k\tau s}+n_\alpha C_{45}^k J_\beta^{k\tau s_z}-n_\beta\frac{1}{R_{\beta k}}C_{44}^k J_{\alpha/\beta}^{k\tau s}+n_\beta C_{44}^k J_\alpha^{k\tau s_z}\\
(\boldsymbol{\Pi}_{uu}^{\tau sk})_{33}&=n_\alpha C_{55}^k J_{\beta/\alpha}^{k\tau s}\partial_\alpha^s+n_\beta C_{44}^k J_{\alpha/\beta}^{k\tau s}\partial_\beta^s+n_\beta C_{45}^k J^{k\tau s}\partial_\alpha^s+n_\alpha C_{45}^k J^{k\tau s}\partial_\beta^s
\end{aligned}\tag{23}$$

One can note that all the equations written for the shell degenerate in those for the plate when $\frac{1}{R_{\alpha k}}=\frac{1}{R_{\beta k}}=0$. In practice, the radii of curvature are set to 10^9.

3.3. Dynamic governing equations

The PVD for the dynamic case is expressed as:

$$\sum_{k=1}^{N_l}\int_{\Omega_k}\int_{A_k}\left\{\delta\epsilon_{pG}^{k\,T}\sigma_{pC}^{k}+\delta\epsilon_{nG}^{k\,T}\sigma_{nC}^{k}\right\}d\Omega_k\,dz$$
$$=\sum_{k=1}^{N_l}\int_{\Omega_k}\int_{A_k}\rho^k\delta\mathbf{u}^{kT}\ddot{\mathbf{u}}^k\,d\Omega_k\,dz+\sum_{k=1}^{N_l}\delta L_e^k \tag{24}$$

where ρ^k is the mass density of the kth layer and double dots denote acceleration.

By substituting the geometrical relations, the constitutive equations and the Unified Formulation, one obtains the following governing equations:

$$\delta\mathbf{u}_s^{k\,T}:\mathbf{K}_{uu}^{k\tau s}\mathbf{u}_\tau^k=\mathbf{M}^{k\tau s}\ddot{\mathbf{u}}_\tau^k+\mathbf{P}_{u\tau}^k \tag{25}$$

In the case of free vibrations one has:

$$\delta\mathbf{u}_s^{k\,T}:\mathbf{K}_{uu}^{k\tau s}\mathbf{u}_\tau^k=\mathbf{M}^{k\tau s}\ddot{\mathbf{u}}_\tau^k \tag{26}$$

where $\mathbf{M}^{k\tau s}$ is the fundamental nucleus for the inertial term. The explicit form of that is:

$$\begin{aligned}
\mathbf{M}_{11}^{k\tau s}&=\rho^k J_{\alpha\beta}^{k\tau s}\\
\mathbf{M}_{12}^{k\tau s}&=0\\
\mathbf{M}_{13}^{k\tau s}&=0\\
\mathbf{M}_{21}^{k\tau s}&=0\\
\mathbf{M}_{22}^{k\tau s}&=\rho^k J_{\alpha\beta}^{k\tau s}\\
\mathbf{M}_{23}^{k\tau s}&=0\\
\mathbf{M}_{31}^{k\tau s}&=0\\
\mathbf{M}_{32}^{k\tau s}&=0\\
\mathbf{M}_{33}^{k\tau s}&=\rho^k J_{\alpha\beta}^{k\tau s}
\end{aligned} \tag{27}$$

where the meaning of the integral $J_{\alpha\beta}^{k\tau s}$ has been illustrated in Eq. (21). The geometrical and mechanical boundary conditions are the same of the static case. Because the static case is only considered, the mass terms will be neglected.

4. The radial basis function method

4.1. The static problem

Radial basis functions (RBF) approximations are mesh-free numerical schemes that can exploit accurate representations of the boundary, are easy to implement and can be spectrally accurate. In this section the formulation of a global unsymmetrical collocation RBF-based method to compute elliptic operators is presented.

Consider a linear elliptic partial differential operator L and a bounded region Ω in $\mathbb{R}^n$ with some boundary $\partial\Omega$. In the static problems, the displacements ($\mathbf{u}$) are computed from the global system of equations

$$\mathscr{L}\mathbf{u}=\mathbf{f}\text{ in }\Omega \tag{28}$$
$$\mathscr{L}_B\mathbf{u}=\mathbf{g}\text{ on }\partial\Omega \tag{29}$$

where $\mathscr{L}$, $\mathscr{L}_B$ are linear operators in the domain and on the boundary, respectively. The right-hand side of (28) and (29) represent the external forces applied on the plate or shell and the boundary conditions applied along the perimeter of the plate or shell, respectively. The PDE (Partial Differential Equation) problem defined in (28) and (29) will be replaced by a finite problem, defined by an algebraic system of equations, after the radial basis expansions.

4.2. The eigenproblem

The eigenproblem looks for eigenvalues (λ) and eigenvectors ($\mathbf{u}$) that satisfy

$$\mathscr{L}\mathbf{u}+\lambda\mathbf{u}=0\text{ in }\Omega \tag{30}$$
$$\mathscr{L}_B\mathbf{u}=0\text{ on }\partial\Omega \tag{31}$$

As in the static problem, the eigenproblem defined in (30) and (31) is replaced by a finite-dimensional eigenvalue problem, based on RBF approximations.

4.3. Radial basis functions approximations

The radial basis function (ϕ) approximation of a function ($\mathbf{u}$) is given by

$$\tilde{\mathbf{u}}(\mathbf{x})=\sum_{i=1}^{N}\alpha_i\phi(\|x-y_i\|_2),\quad\mathbf{x}\in\mathbb{R}^n \tag{32}$$

where y_i, $i=1,\ldots,N$ is a finite set of distinct points (centers) in $\mathbb{R}^n$. The most common RBFs are

$$\begin{aligned}
&\text{Cubic}: && \phi(r)=r^3\\
&\text{Thin plate splines}: && \phi(r)=r^2\log(r)\\
&\text{Wendland functions}: && \phi(r)=(1-r)_+^m p(r)\\
&\text{Gaussian}: && \phi(r)=e^{-(cr)^2}\\
&\text{Multiquadrics}: && \phi(r)=\sqrt{c^2+r^2}\\
&\text{Inverse multiquadrics}: && \phi(r)=(c^2+r^2)^{-1/2}
\end{aligned}$$

where the Euclidian distance r is real and non-negative and c is a positive shape parameter. Hardy [45] introduced multiquadrics in the analysis of scattered geographical data. In the 1990s Kansa [26] used multiquadrics for the solution of partial differential equations. Considering N distinct interpolations, and knowing $u(x_j)$, $j=1,2,\ldots,N$, one finds α_i by the solution of a $N\times N$ linear system

$$\mathbf{A}\boldsymbol{\alpha}=\mathbf{u} \tag{33}$$

where $\mathbf{A}=[\phi(\|x-y_i\|_2)]_{N\times N}$, $\boldsymbol{\alpha}=[\alpha_1,\alpha_2,\ldots,\alpha_N]^T$ and $\mathbf{u}=[u(x_1),u(x_2),\ldots,u(x_N)]^T$.

4.4. Solution of the static problem

The solution of a static problem by radial basis functions considers N_I nodes in the domain and N_B nodes on the boundary, with a total number of nodes $N=N_I+N_B$. One can denote the sampling points by $x_i\in\Omega$, $i=1,\ldots,N_I$ and $x_i\in\partial\Omega$, $i=N_I+1,\ldots,N$. At the points in the domain, the following system of equations is solved

$$\sum_{i=1}^{N}\alpha_i\mathscr{L}\phi(\|x-y_i\|_2)=\mathbf{f}(x_j),\quad j=1,2,\ldots,N_I \tag{34}$$

or

$$\mathscr{L}^I\boldsymbol{\alpha}=\mathbf{F} \tag{35}$$

where

$$\mathscr{L}^I=[\mathscr{L}\phi(\|x-y_i\|_2)]_{N_I\times N} \tag{36}$$

At the points on the boundary, the following boundary conditions are imposed

$$\sum_{i=1}^{N}\alpha_i\mathscr{L}_B\phi(\|x-y_i\|_2)=\mathbf{g}(x_j),\quad j=N_I+1,\ldots,N \tag{37}$$

or

$$\mathbf{B}\boldsymbol{\alpha}=\mathbf{G} \tag{38}$$

where

$$\mathbf{B} = \mathscr{L}_B\phi\left[\left(\|x_{N_I+1} - y_j\|_2\right)\right]_{N_B\times N}$$

Therefore, one can write a finite-dimensional static problem as

$$\begin{bmatrix}\mathscr{L}^I\\ \mathbf{B}\end{bmatrix}\boldsymbol{\alpha} = \begin{bmatrix}\mathbf{F}\\ \mathbf{G}\end{bmatrix} \tag{39}$$

By inverting the system (39), one obtains the vector $\boldsymbol{\alpha}$. Then, the solution $\mathbf{u}$ is calculated using the interpolation Eq. (32).

4.5. Solution of the eigenproblem

Consider N_I nodes in the interior of the domain and N_B nodes on the boundary, with $N = N_I + N_B$. The interpolation points are denoted by $x_i \in \Omega$, $i = 1,\ldots,N_I$ and $x_i \in \partial\Omega$, $i = N_I + 1,\ldots,N$. At the points in the domain, the following eigenproblem is defined

$$\sum_{i=1}^{N}\alpha_i\mathscr{L}\phi(\|x - y_i\|_2) = \lambda\tilde{\mathbf{u}}(x_j), j = 1,2,\ldots,N_I \tag{40}$$

or

$$\mathscr{L}^I\boldsymbol{\alpha} = \lambda\tilde{\mathbf{u}}^I \tag{41}$$

where

$$\mathscr{L}^I = [\mathscr{L}\phi(\|x - y_i\|_2)]_{N_I\times N} \tag{42}$$

At the points on the boundary, the imposed boundary conditions are

$$\sum_{i=1}^{N}\alpha_i\mathscr{L}_B\phi(\|x - y_i\|_2) = 0, \quad j = N_I + 1,\ldots,N \tag{43}$$

or

$$\mathbf{B}\boldsymbol{\alpha} = 0 \tag{44}$$

Eqs. (41) and (44) can now be solved as a generalized eigenvalue problem

$$\begin{bmatrix}\mathscr{L}^I\\ \mathbf{B}\end{bmatrix}\boldsymbol{\alpha} = \lambda\begin{bmatrix}\mathbf{A}^I\\ \mathbf{0}\end{bmatrix}\boldsymbol{\alpha} \tag{45}$$

where

$$\mathbf{A}^I = \phi\left[\left(\|x_{N_I} - y_j\|_2\right)\right]_{N_I\times N}$$

4.6. Discretization of the equations of motion and boundary conditions

The radial basis collocation method follows a simple implementation procedure. Taking Eq. (39), one computes

$$\boldsymbol{\alpha} = \begin{bmatrix}L^I\\ \mathbf{B}\end{bmatrix}^{-1}\begin{bmatrix}\mathbf{F}\\ \mathbf{G}\end{bmatrix} \tag{46}$$

This $\boldsymbol{\alpha}$ vector is then used to obtain solution $\tilde{\mathbf{u}}$, by using (32). If derivatives of $\tilde{\mathbf{u}}$ are needed, such derivatives are computed as

$$\frac{\partial\tilde{\mathbf{u}}}{\partial x} = \sum_{j=1}^{N}\alpha_j\frac{\partial\phi_j}{\partial x} \tag{47}$$

$$\frac{\partial^2\tilde{\mathbf{u}}}{\partial x^2} = \sum_{j=1}^{N}\alpha_j\frac{\partial^2\phi_j}{\partial x^2}, \text{ etc.} \tag{48}$$

In the present collocation approach, one needs to impose essential and natural boundary conditions. Consider, for example, the condition $w = 0$, on a simply supported or clamped edge. The conditions are enforced by interpolating as

$$w = 0 \rightarrow \sum_{j=1}^{N}\alpha_j^W\phi_j = 0 \tag{49}$$

Other boundary conditions are interpolated in a similar way.

4.7. Free vibrations problems

For free vibration problems, the external forces are set to zero, and an harmonic solution is assumed for the displacements u_0, u_1, v_0, v_1,...

$$u_0 = U_0(x,y)e^{i\omega t}; \quad u_1 = U_1(x,y)e^{i\omega t}; \quad u_3 = U_3(x,y)e^{i\omega t} \tag{50}$$

$$v_0 = V_0(x,y)e^{i\omega t}; \quad v_1 = V_1(x,y)e^{i\omega t}; \quad v_3 = V_3(x,y)e^{i\omega t} \tag{51}$$

$$w_0 = W_0(x,y)e^{i\omega t}; \quad w_1 = W_1(x,y)e^{i\omega t}; \quad w_3 = W_3(x,y)e^{i\omega t} \tag{52}$$

where ω is the frequency of natural vibration. Substituting the harmonic expansion into Eq. (45) in terms of the amplitudes U_0, U_1, U_3, V_0, V_1, V_3, W_0, W_1, W_3, one can obtain the natural frequencies and vibration modes for the plate or shell problem, by solving the eigenproblem

$$\left[\mathscr{L} - \omega^2\mathscr{G}\right]\mathbf{X} = \mathbf{0} \tag{53}$$

where $\mathscr{L}$ collects all stiffness terms and $\mathscr{G}$ collects all terms related to the inertial terms. In (53) $\mathbf{X}$ are the modes of vibration associated with the natural frequencies defined as ω.

5. Numerical examples

All numerical examples consider a Chebyshev grid (see Fig. 3) and a Wendland function, defined as

$$\phi(r) = (1 - cr)_+^8\left(32(cr)^3 + 25(cr)^2 + 8cr + 1\right) \tag{54}$$

where the shape parameter (c) was obtained by an optimization procedure, as detailed in Ferreira and Fasshauer [46].

5.1. Spherical shell in bending

A laminated composite spherical shell is here considered, of side a and thickness h, composed of layers oriented at [0°/90°/0°]

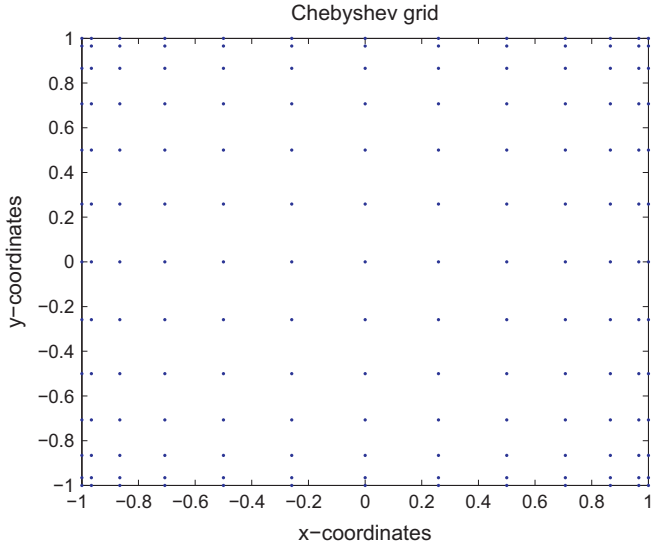

Fig. 3. A sketch of a Chebyshev grid for 13 × 13 points.

Table 1
Non-dimensional central deflection, $\bar{w} = w\frac{10^2 E_2 h^3}{P_0 a^4}$ variation with various number of grid points per unit length, N for different R/a ratios, for $R_1 = R_2$.

	a/h	Method	R/a					
			5	10	20	50	100	10^9
[0°/90°/0°]	10	Present (13 × 13)	6.6874	6.9044	6.9615	6.9781	6.9806	6.9816
	10	Present (17 × 17)	6.6879	6.9047	6.9618	6.9784	6.9809	6.9819
	10	Present (21 × 21)	6.6880	6.9048	6.9618	6.9784	6.9809	6.9820
	10	HSDT [47]	6.7688	7.0325	7.1016	7.1212	7.1240	7.125
	10	FSDT [47]	6.4253	6.6247	6.6756	6.6902	6.6923	6.6939
	100	Present (13 × 13)	1.0244	2.3651	3.5151	4.0692	4.1629	4.1951
	100	Present (17 × 17)	1.0249	2.3661	3.5165	4.0707	4.1644	4.1966
	100	Present (21 × 21)	1.0250	2.3662	3.5167	4.0709	4.1646	4.1966
	100	HSDT [47]	1.0321	2.4099	3.617	4.2071	4.3074	4.3420
	100	FSDT [47]	1.0337	2.4109	3.6150	4.2027	4.3026	4.3370
[0°/90°/90°/0°]	10	Present (13 × 13)	6.7199	6.9418	7.0004	7.0174	7.0201	7.0211
	10	Present (17 × 17)	6.7204	6.9423	7.0007	7.0178	7.0204	7.0214
	10	Present (21 × 21)	6.7205	6.9423	7.0008	7.0178	7.0204	7.0215
	10	HSDT [47]	6.7865	7.0536	7.1237	7.1436	7.1464	7.1474
	10	FSDT [47]	6.3623	6.5595	6.6099	6.6244	6.6264	6.6280
	100	Present (13 × 13)	1.0190	2.3581	3.5119	4.0694	4.1638	4.1962
	100	Present (17 × 17)	1.0195	2.3591	3.5132	4.0708	4.1653	4.1978
	100	Present (21 × 21)	1.0195	2.3592	3.5134	4.0711	4.1655	4.1980
	100	HSDT [47]	1.0264	2.4024	3.6133	4.2071	4.3082	4.3430
	100	FSDT [47]	1.0279	2.4030	3.6104	4.2015	4.3021	4.3368

Table 2
Nondimensionalized fundamental frequencies of cross-ply laminated spherical shells, $\bar{\omega} = \omega\frac{a^2}{h}\sqrt{\rho/E_2}$, laminate ([0°/90°/90°/0°]).

a/h	Method	R/a					
		5	10	20	50	100	10^9
10	Present (13 × 13)	12.0999	11.9378	11.8967	11.8851	11.8835	11.8829
	Present (17 × 17)	12.0995	11.9375	11.8964	11.8849	11.8832	11.8827
	Present (21 × 21)	12.0994	11.9375	11.8964	11.8849	11.8832	11.8827
	HSDT [47]	12.040	11.840	11.790	11.780	11.780	11.780
100	Present (13 × 13)	31.2175	20.5753	16.8713	15.6760	15.4977	15.4378
	Present (17 × 17)	31.2076	20.5690	16.8663	15.6714	15.4931	15.4333
	Present (21 × 21)	31.2063	20.5683	16.8658	15.6711	15.4929	15.4331
	HSDT [47]	31.100	20.380	16.630	15.420	15.230	15.170

Table 3
Nondimensionalized fundamental frequencies of cross-ply laminated spherical shells, $\bar{\omega} = \omega\frac{a^2}{h}\sqrt{\rho/E_2}$, laminate ([0°/90°/0°]).

a/h	Method	R/a					
		5	10	20	50	100	10^9
10	Present (13 × 13)	12.1258	11.9661	11.9256	11.9142	11.9126	11.9120
	Present (17 × 17)	12.1254	11.9658	11.9253	11.9140	11.9123	11.9112
	Present (21 × 21)	12.1253	11.9658	11.9253	11.9140	11.9123	11.9112
	HSDT [47]	12.060	11.860	11.810	11.790	11.790	11.790
100	Present (13 × 13)	31.1360	20.5441	16.8634	15.6764	15.4993	15.4398
	Present (17 × 17)	31.1262	20.5388	16.8584	15.6718	15.4948	15.4353
	Present (21 × 21)	31.1249	20.5381	16.8579	15.6714	15.4944	15.4349
	HSDT [47]	31.020	20.350	16.620	15.420	15.240	15.170

and [0°/90°/90°/0°]. The shell is subjected to a sinusoidal vertical pressure of the form

$$p_z = P\sin\left(\frac{\pi x}{a}\right)\sin\left(\frac{\pi y}{a}\right)$$

with the origin of the coordinate system located at the lower left corner on the midplane and P the maximum load (at center of shell).

The orthotropic material properties for each layer are given by

$$E_1 = 25.0E_2, \quad G_{12} = G_{13} = 0.5E_2, \quad G_{23} = 0.2E_2, \quad \nu_{12} = 0.25$$

The in-plane displacements, the transverse displacements, the normal stresses and the in-plane and transverse shear stresses are presented in normalized form as

$$\bar{w} = \frac{10^3 w_{(a/2,a/2,0)} h^3 E_2}{Pa^4}, \quad \bar{\sigma}_{xx} = \frac{\sigma_{xx(a/2,a/2,h/2)} h^2}{Pa^2}, \quad \bar{\sigma}_{yy} = \frac{\sigma_{yy(a/2,a/2,h/4)} h^2}{Pa^2}, \quad \bar{\tau}_{xz} = \frac{\tau_{xz(0,a/2,0)} h}{Pa}, \quad \bar{\tau}_{xy} = \frac{\tau_{xy(0,0,h/2)} h^2}{Pa^2}$$

The shell is simply supported on all edges.

In Table 1, the static deflections for the present shell model are compared with results of Reddy shell formulation using first-order and third-order shear deformation theories [47]. Nodal grids with 13 × 13, 17 × 17, and 21 × 21 points are considered. Various values of R/a and two values of a/h (10 and 100) are taken for the analysis. Results are in good agreement for various a/h ratios with the higher-order results of Reddy [47].

Table 4
Nondimensionalized fundamental frequencies of cross-ply cylindrical shells, $\bar{\omega} = \omega \frac{a^2}{h}\sqrt{\rho/E_2}$.

R/a	Method	[0/90/0]		[0/90/90/0]	
		a/h = 100	a/h = 10	a/h = 100	a/h = 10
5	Present (13 × 13)	20.4988	11.9234	20.5310	11.9010
	Present (17 × 17)	20.4871	11.9230	20.5214	11.9007
	Present (21 × 21)	20.4856	11.9230	20.5202	11.9007
	FSDT [47]	20.332	12.207	20.361	12.267
	HSDT [47]	20.330	11.850	20.360	11.830
10	Present (13 × 13)	16.8448	11.9149	16.8598	11.8874
	Present (17 × 17)	16.8448	11.9146	16.8538	11.8872
	Present (21 × 21)	16.8441	11.9146	16.8531	11.8872
	FSDT [47]	16.625	12.173	16.634	12.236
	HSDT [47]	16.620	11.800	16.630	11.790
20	Present (13 × 13)	15.8048	11.9127	15.8055	11.8840
	Present (17 × 17)	15.7998	11.9125	15.8006	11.8838
	Present (21 × 21)	15.7993	11.9125	15.8001	11.8838
	FSDT [47]	15.556	12.166	15.559	12.230
	HSDT [47]	15.55	11.79	15.55	11.78
50	Present (13 × 13)	15.4988	11.9121	15.4972	11.8831
	Present (17 × 17)	15.4942	11.9119	15.4926	11.8829
	Present (21 × 21)	15.4938	11.9119	15.4922	11.8829
	FSDT [47]	15.244	12.163	15.245	12.228
	HSDT [47]	15.24	11.79	15.23	11.78
100	Present (13 × 13)	15.4546	11.9120	15.4527	11.8830
	Present (17 × 17)	15.4501	11.9118	15.4481	11.8827
	Present (21 × 21)	15.4497	11.9118	15.4477	11.8827
	FSDT [47]	15.198	12.163	15.199	12.227
	HSDT [47]	15.19	11.79	15.19	11.78
Plate	Present (13 × 13)	15.4398	11.9120	15.4378	11.8829
	Present (17 × 17)	15.4353	11.9118	15.4333	11.8827
	Present (21 × 21)	15.4349	11.9118	15.4328	11.9927
	FSDT [47]	15.183	12.162	15.184	12226
	HSDT [47]	15.170	11.790	15.170	11.780

5.2. Free vibration of spherical and cylindrical laminated shells

Nodal grids with 13 × 13, 17 × 17, and 21 × 21 points are considered. In Tables 2 and 3 the nondimensionalized natural frequencies from the present SSDT theory for various cross-ply spherical shells are compared with analytical solutions by Reddy and Liu [47], who considered both the First-order Shear Deformation Theory (FSDT) and the High-order Shear Deformation Theory (HSDT). The first-order theory overpredicts the fundamental natural frequencies of symmetric thick shells and symmetric shallow thin shells. The present radial basis function method is compared with analytical results by Reddy [47] and shows excellent agreement.

Table 4 contain nondimensionalized natural frequencies obtained using the present SSDT theory for cross-ply cylindrical shells with lamination schemes [0/90/0], [0/90/90/0]. Present results are compared with analytical solutions by Reddy and Liu [47] who considered both the first-order (FSDT) and the third-order (HSDT) theories. The present radial basis function method is compared with analytical results by Reddy [47] and shows excellent agreement.

In Fig. 4, the first four vibrational modes of cross-ply laminated spherical shells, $\bar{\omega} = \omega \frac{a^2}{h}\sqrt{\rho/E_2}$, are illustrated for a laminate ([0°/90°/90°/0°]), using a grid of 13 × 13 points, for a/h = 100, R/a = 10. The modes of vibration are quite stable.

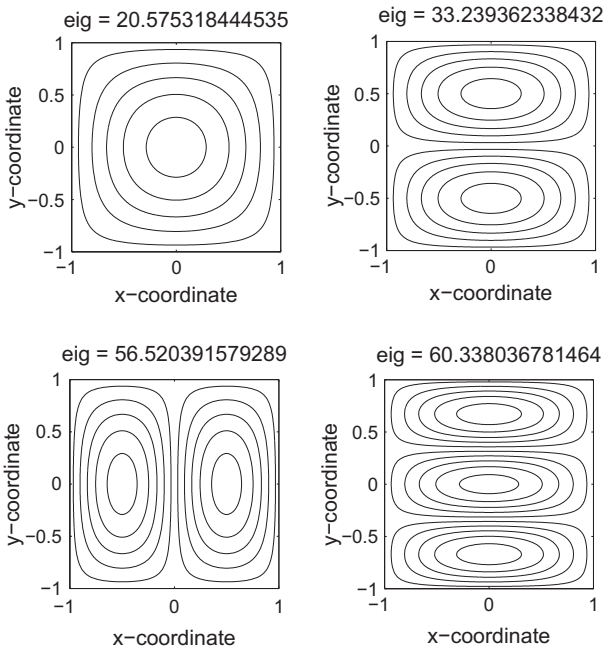

Fig. 4. First four vibrational modes of cross-ply laminated spherical shells, $\bar{\omega} = \omega \frac{a^2}{h}\sqrt{\rho/E_2}$, laminate ([0°/90°/90°/0°]) grid 13 × 13 points, a/h = 100,R/a = 10.

6. Concluding remarks

In this paper a sinusoidal shear deformation theory was implemented for the first time for laminated orthotropic elastic shells through a multiquadrics discretization of equations of motion and boundary conditions. The multiquadric radial basis function method for the solution of shell bending and free vibration problems was presented. Results for static deformations and natural frequencies were obtained and compared with other sources. This meshless approach demonstrated that is very successful in the static deformations and free vibration analysis of laminated compos-

ite shells. Advantages of radial basis functions are absence of mesh, ease of discretization of boundary conditions and equations of equilibrium or motion and very easy coding. The static displacements and the natural frequencies obtained from present method are shown to be in excellent agreement with analytical solutions.

Acknowledgements

The support of Ministério da Ciência Tecnologia e do Ensino superior and Fundo Social Europeu (MCTES and FSE) under programs POPH-QREN are gratefully acknowledged.

References

[1] Koiter WT. On the foundations of the linear theory of thin elastic shell. Proc Kon Ned Akad Wetensch 1970;73:169–95.
[2] Naghdi PM. A survey of recent progress in the theory of elastic shells. Appl Mech Rev 1956;9:365–8.
[3] Carrera E. Developments, ideas, and evaluations based upon reissner's mixed variational theorem in the modelling of multilayered plates and shells. Appl Mech Rev 2001;54:301–29.
[4] Carrera E. Theories and finite elements for multilayered plates and shells: a unified compact formulation with numerical assessment and benchmarking. Arch Comput Methods Eng 2003;10:215–96.
[5] Carrera E. On the use of the Murakami's zig-zag function in the modeling of layered plates and shells. Comput Struct 2004;82:541–54.
[6] Carrera E, Brischetto S. Analysis of thickness locking in classical, refined and mixed theories for layered shells. Compos Struct 2008;85:83–90.
[7] Cinefra M, Belouettar S, Soave M, Carrera E. Variable kinematic models applied to free-vibration analysis of functionally graded material shells. Eur J Mech A/Solids 2010;29:1078–87.
[8] D'Ottavio M, Ballhause D, Kröplin B, Carrera E. Closed-form solutions for the free-vibration problem of multilayered piezoelectric shells. Comput Struct 2006;84:1506–18.
[9] Touratier M. A generalization of shear deformation theories for axisymmetric multilayered shells. Int J Solids Struct 1992;29:1379–99.
[10] Touratier M. An efficient standard plate theory. Int J Eng Sci 1991;29:901–16.
[11] Touratier M. A refined theory of laminated shallow shells. Int J Solids Struct 1992;29:1401–15.
[12] Vidal P, Polit O. A family of sinus finite elements for the analysis of rectangular laminated beams. Compos Struct 2008;84:56–72.
[13] Cheng S. Elasticity theory of plates and a refined theory. J Appl Mech 1979;46:644–50.
[14] Polit O, Touratier M. High order triangular sandwich plate finite element for linear and nonlinear analyses. Comput Methods Appl Mech Eng 2000;185:305–24.
[15] Chapelle D, Bathe K-J. The finite element analysis of shells: fundamentals. Berlin: Springer; 2003.
[16] Flügge W. Stresses in shells. 2nd ed. Berlin: Springer; 1960.
[17] Scordelis A, Lo KS. Computer analysis in cylindrical shells. J Am Concr Inst 1964;61:561–93.
[18] Reddy JN. Mechanics of laminated composite plates and shells. Theory and analysis. FL: CRC Press; 2003.
[19] Carrera E. Theories and finite elements for multilayered plates and shells: a unified compact formulation with numerical assessment and benchmarking. Arch Comput Methods Eng 2003;10:215–96.
[20] Pitkäranta J. The problem of membrane locking in finite element analysis of cylindrical shells. Numer Math 1992;61:523–42.
[21] Chinosi C, Della Croce L, Scapolla T. Numerical results on the locking for cylindrical shells. Comput-Assist Mech Eng Sci J 1998;5(1):31–44.
[22] Zienkiewicz 0C, Taylor RL, Too JM. Reduced integration techniques in general analysis of plates and shells. Int J Numer Methods Eng 1971;3:275–90.
[23] Bathe K-J, Dvorkin E. A formulation of general shell elements – the use of mixed interpolation of tensorial components. Int J Numer Methods Eng 1986;22:697–722.
[24] Arnold DN, Brezzi F. Locking free finite element methods for shells. Math Comput 1997;66:1–14.
[25] Huang H-C. Membrane locking and assumed strain shell elements. Comput Struct 1987;27(5):671–7.
[26] Kansa EJ. Multiquadrics – a scattered data approximation scheme with applications to computational fluid dynamics. I: Surface approximations and partial derivative estimates. Comput Math Appl 1990;19(8/9):127–45.
[27] Hon YC, Lu MW, Xue WM, Zhu YM. Multiquadric method for the numerical solution of biphasic mixture model. Appl Math Comput 1997;88:153–75.
[28] Hon YC, Cheung KF, Mao XZ, Kansa EJ. A multiquadric solution for the shallow water equation. ASCE J Hydraul Eng 1999;125(5):524–33.
[29] Wang JG, Liu GR, Lin P. Numerical analysis of Biot's consolidation process by radial point interpolation method. Int J Solids Struct 2002;39(6):1557–73.
[30] Liu GR, Gu YT. A local radial point interpolation method (LRPIM) for free vibration analyses of 2-d solids. J Sound Vib 2001;246(1):29–46.
[31] Liu GR, Wang JG. A point interpolation meshless method based on radial basis functions. Int J Numer Methods Eng 2002;54:1623–48.
[32] Wang JG, Liu GR. On the optimal shape parameters of radial basis functions used for 2-d meshless methods. Comput Methods Appl Mech Eng 2002;191:2611–30.
[33] Chen XL, Liu GR, Lim SP. An element free Galerkin method for the free vibration analysis of composite laminates of complicated shape. Compos Struct 2003;59:279–89.
[34] Dai KY, Liu GR, Lim SP, Chen XL. An element free Galerkin method for static and free vibration analysis of shear-deformable laminated composite plates. J Sound Vib 2004;269:633–52.
[35] Liu GR, Chen XL. Buckling of symmetrically laminated composite plates using the element-free Galerkin method. Int J Struct Stab Dyn 2002;2:281–94.
[36] Liew KM, Chen XL, Reddy JN. Mesh-free radial basis function method for buckling analysis of non-uniformity loaded arbitrarily shaped shear deformable plates. Comput Methods Appl Mech Eng 2004;193:205–25.
[37] Q Huang Y, Li QS. Bending and buckling analysis of antisymmetric laminates using the moving least square differential quadrature method. Comput Methods Appl Mech Eng 2004;193:3471–92.
[38] Liu L, Liu GR, Tan VCB. Element free method for static and free vibration analysis of spatial thin shell structures. Comput Methods Appl Mech Eng 2002;191:5923–42.
[39] Xiang S, Wang KM, Ai YT, Sha YD, Shi H. Analysis of isotropic, sandwich and laminated plates by a meshless method and various shear deformation theories. Compos Struct 2009;91(1):31–7.
[40] Xiang S, Shi H, Wang KM, Ai YT, Sha YD. Thin plate spline radial basis functions for vibration analysis of clamped laminated composite plates. Eur J Mech A/Solids 2010;29:844–50.
[41] Ferreira AJA, Roque CMC, Jorge RMN. Analysis of composite and sandwich plate by trigonometric layer-wise deformation theory and radial basis function. J Sandwich Struct Mater 2006;8:497–515.
[42] Ferreira AJM. A formulation of the multiquadric radial basis function method for the analysis of laminated composite plates. Compos Struct 2003;59:385–92.
[43] Ferreira AJM. Thick composite beam analysis using a global meshless approximation based on radial basis functions. Mech Adv Mater Struct 2003;10:271–84.
[44] Ferreira AJM, Roque CMC, Martins PALS. Analysis of composite plates using higher-order shear deformation theory and a finite point formulation based on the multiquadric radial basis function method. Composites: Part B 2003;34:627–36.
[45] Hardy RL. Multiquadric equations of topography and other irregular surfaces. Geophys Res 1971;176:1905–15.
[46] Ferreira AJM, Fasshauer GE. Computation of natural frequencies of shear deformable beams and plates by a RBF-pseudospectral method. Comput Methods Appl Mech Eng 2006;196:134–46.
[47] Reddy JN, Liu CF. A higher-order shear deformation theory of laminated elastic shells. Int J Eng Sci 1985;23:319–30.